Self-assembly of ink molecules in dip-pen nanolithography: A diffusion model

Joonkyung Jang, Seunghun Hong, George C. Schatz, and Mark A. Ratner

Citation: The Journal of Chemical Physics **115**, 2721 (2001);
View online: https://doi.org/10.1063/1.1384550
View Table of Contents: http://aip.scitation.org/toc/jcp/115/6
Published by the American Institute of Physics

Self-assembly of ink molecules in dip-pen nanolithography: A diffusion model

Joonkyung Jang, Seunghun Hong, George C. Schatz, and Mark A. Ratner
Department of Chemistry, Materials Research Center and Center for Nanofabrication and Molecular Self-Assembly, Northwestern University, Evanston, Illinois 60208

(Received 12 March 2001; accepted 17 May 2001)

The self-assembly of ink molecules deposited using dip-pen nanolithography (DPN) is modeled as a two-dimensional diffusion with a source (tip). A random walk simulation and simple analytic theory are used to study how the diffusion dynamics affects patterns generated in DPN. For a tip generating a constant flux of ink molecules, circles, lines, and letters are studied by varying the deposition rate of ink molecules and the tip scan speed. Even under the most favorable condition studied here, peripheries of patterns fluctuate from perfect circles or lines, due to the random, diffusional nature of self-assembly. The degree of fluctuation is quantified for circles and lines. Circles generated by fixing the tip position do not depend on the deposition rate if the same amount of ink is deposited. For a moving tip, patterns change drastically depending on tip speed and deposition rate. Overall, fast scan or slow deposition relative to the diffusion time scale makes lines narrower. When the tip deposits ink too slowly or scans too fast, patterns become incoherent, making molecules in patterns separated from each other. Therefore, there seems to be an optimal choice of the deposition rate and tip speed that gives both narrow and coherent patterns. We also explore the consequences of varying the relative rates of diffusion of ink molecules on bare surface and on previously deposited molecules.
[DOI: 10.1063/1.1384550]

I. INTRODUCTION

Dip-pen nanolithography (DPN) (Refs. 1–4) has emerged as a promising tool for constructing nanostructures on surfaces. With the use of an atomic force microscopy (AFM) tip coated with molecular ink (i.e., alkanethiol), one can transfer ink molecules to a substrate surface (i.e., gold) and draw patterns with nanoscale resolution. There is some evidence that the ink transport from the tip is mediated by a water meniscus that forms between the tip and the surface under atmospheric conditions.[4,5] The success of DPN relies on two factors: a spatially narrow *deposition* of ink molecules from the tip and *self-assembly* of the ink molecules functionalized to chemisorb to the substrate and to form a compact monolayer on the surface.

Exactly how DPN works is largely unknown, leading to questions such as: What is the ultimate resolution of DPN? How sensitive is it to temperature and humidity? The deposition of ink is required for DPN, but the whole process ends only after the molecules move across the surface and finally are trapped by adsorbing sites of the substrate. It is the latter aspect of DPN that we would like to focus on in this paper. We take the molecular flow from the tip as given, and study how molecules diffuse and self-assemble to form patterns after deposition.

The model we propose for the self-assembly involves diffusion of ink molecules on a two-dimensional lattice with trapping sites (Fig. 1). Let us consider the simplest case where the ink is deposited from a tip fixed in position. To mimic the strong chemical bond between the substrate and ink molecule in DPN, we assume molecules become immediately trapped and are immobile once they reach one of the chemisorbing bare metal sites on the surface. Then the molecules deposited earlier in time will be likely to be adsorbed sooner than the later ones. And molecules deposited later in time, finding the chemisorbing sites near the tip already occupied by molecules deposited earlier, have to travel farther to reach previously unoccupied trapping sites. Due to the finite mobility of the ink molecules, the area around the tip could be congested depending on how fast molecules are deposited from the tip. The transport then can be thought of as being driven by the concentration gradient from the high density region (around the tip) to the zero coverage region (unoccupied trapping sites). The above argument suggests that, at least phenomenologically, DPN can be viewed as a diffusion with a source (tip).

With this diffusional picture of the self-assembly, what becomes important is the relative time scale of diffusion with respect to that of deposition. If diffusion is much faster than deposition, adsorption might occur in a one-molecule-at-a-time fashion. But if the reverse is true, the transport would involve simultaneous diffusion of many molecules. It has been recognized that molecular diffusion in self-assembly limits[7] the resolution of microcontact printing (μCP),[8,9] where the patterns are deposited through an elastomer stamp. In contrast to the parallel nature of μCP, DPN is a serial lithographic technique. In order to generate patterns in DPN, one needs to move the tip across the surface. Then a significant issue is how the relative tip speed compared to the diffusion time scale affects properties of patterns.

In this paper, we adopt a random walk simulation to

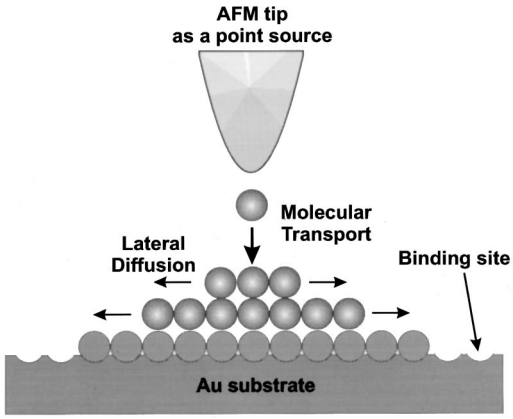

FIG. 1. Proposed transport mechanism of ink molecules from the tip to the substrate. The incoming molecular flux from the tip creates a concentration gradient around the tip, and ink molecules subsequently diffuse over the region already occupied by other ink molecules (drawn as filled circles) to be finally trapped by the bare surface of the substrate.

study how the patterns change as we vary the time scales of deposition and tip scan relative to that of diffusion. We discuss the qualitative behavior of circles, lines, and letters with respect to variation of these variables. To compare our simulation with a specific experiment, the diffusivity needs to be identified. We use earlier measurement of diffusion constants to provide estimate of the relevant time scales in DPN.

It should be noted that our model assumes two distinct regions in which the dynamics of self-assembly occur; molecules diffuse only over the region already covered by other molecules and are immediately trapped by any contact with the bare surface. Thus the conventional surface diffusivity with which adsorbates diffuse over the bare surfaces[10] is taken to be zero. Then the growth of patterns can be thought of as the growth of a phase with a finite diffusivity in contact with a phase with zero diffusivity. With this notion, our model poses a new type of phase growth problem.[11,12] We show that the growth of circles in our model reduces to the well known problem of the phase growth in diffusion theory. A simple analytic theory is derived for the circle growth and shown to agree well with simulation. We also consider simulations in which the diffusivity on bare surface is nonzero.

This paper is organized as follows: In Sec. II, we present simulation details for the random walk on a square lattice. A continuum theory for circle growth generated by a fixed tip is given in Sec. III. Results from simulation and the continuum theory are reported in Sec. IV; circles from simulation are compared with those from the analytic theory, and their noncircularities are analyzed. We then move on to a tip moving with various speeds, and examine lines and letters formed by varying deposition rates. We summarize and conclude in Sec. V.

II. DETAILS OF RANDOM WALK SIMULATION

A two-dimensional (2D) random walk simulation with discrete step and time has been performed to emulate typical DPN experiments: random walks are allowed between the sites on a square lattice with a grid length l and a time interval Δt. Note that, to conform to 2D diffusion picture, Δt and l should satisfy

$$4D\Delta t = l^2. \tag{2.1}$$

Every site on the lattice is assumed to trap ink molecules; thus, if a molecule arrives at a site previously unoccupied by other molecules, it is trapped. If the site is already occupied, molecules are free to continue walking. This way, the diffusion takes place only in a region where a monolayer of trapped ink molecules exists. In light of the isotropic flow of ink over the surface observed in DPN experiments,[4] the random walk is taken to be directionally isotropic: for a given lattice position of a walker, (x,y), the random jump is made (if it is allowed) with equal probability to one of its four nearest neighbor sites, $(x+l,y)$, $(x-l,y)$, $(x,y+l)$, and $(x,y-l)$.

When more than two molecules occupy the same lattice site during simulation, the order in time at which each molecule has arrived at that site has been tracked. And the walker that arrived later is given a higher vertical position on the site, and the molecules are stacked from bottom up in the increasing order of their arrival times (i.e., if there are three molecules on a lattice site, we assign vertical positions 1, 2, and 3 to molecules in the ascending order of their arrival times). For each walker, the excluded volume effect due to its four neighboring molecules is taken into account as follows. For every random jump of a walker, the jump is accepted only if the current vertical position of the walker is higher than the highest vertical position of the site it jumps to. With this scheme, molecules are moved sequentially for every time step. Since the sequence now is important due to the excluded volume effect, we randomly choose the order in which each molecule moves. After each random jump, we made sure every site is stacked properly from bottom up. If a site is not properly stacked (i.e., a site is occupied by molecules with vertical positions 1, 2, and 3, and then molecule with vertical position 2 jumps to another site), the vertical positions of molecules on the site are adjusted. To assess the importance of the excluded volume effect, we also ran a simulation without such effect and compared it with the full simulation.

The source of ink, that is the tip, is allowed to move between the discrete sites on the lattice. A range of tip scan velocity v relative to the diffusion velocity, $v^*=v/(l/\Delta t)$, has been studied. For a tip moving slowly, $v^*<1$, the tip is displaced by one grid length for every $1/v^*$ time step ($1/v^*$ is chosen to be an integer). When $v^*>1$, the tip moves v^* grid points per time step. To generate a variety of patterns, it is necessary to move the tip diagonally or in a direction other than x or y. In this case, the tip position could end up not being on one of the square lattice points. When that happens, the ink molecules are deposited at the sites nearest to the tip.

In Fig. 2 are shown the radii of circles generated for various contact times between the tip and a polycrystalline gold surface. The radius is measured after octadecanethiols (ODT) deposited by the tip form a monolayer on the gold surface at room temperature and under atmospheric condition.[6] The inset for the figure shows representative

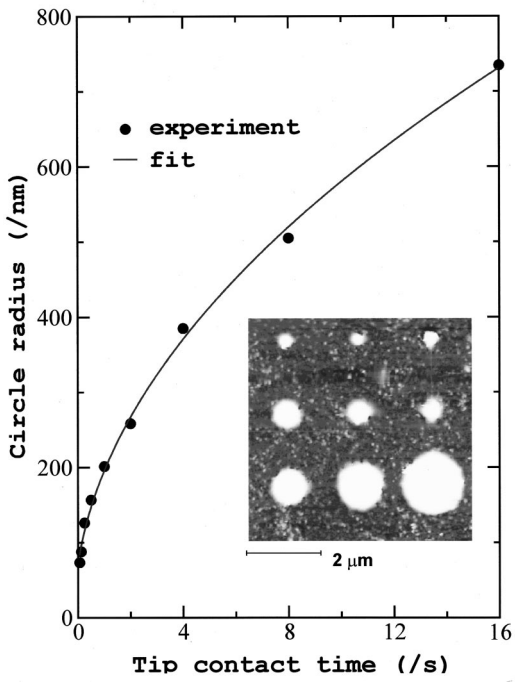

FIG. 2. Circle radius vs contact time of the tip for ODT on a gold surface [10 nm thick polycrystalline gold surface prepared on top of single crystalline Si(100) wafers coated with 5 nm of Ti]. Each circle (monolayer thick ODT) in the inset was formed by putting an AFM tip coated with ODT in contact with the surface for a certain time specified as contact time. The experimental circle radii are estimated from the AFM image (inset) taken after chemically etching the ODT covered Au/Ti/Si substrate. The circle areas covered with ODT survive the etching. See Ref. 6 for more details. The fit in the figure is obtained by fitting the experimental circle area to a linear function of contact time, $A_i = a + b\tau_i$, where A_i and τ_i are the area and contact time for each data point, respectively. The average deviation of 9 data points from the fit, defined as $(1/9)\Sigma_{i=1}^{9}|(A_i - a - b\tau_i)/A_i|$, is found to be 0.12.

DPN results from which the radius is determined. Also drawn in the figure is the fit obtained by approximating the circle area growth as a linear function of contact time.[13] The quality of fit tells us that the number of ink molecules deposited per unit time is well represented by a constant, n, for the experimental time scale. Assuming the density of ODT on the gold surface to be the monolayer density of ODT on Au(111) (approximately 1/25 Å^2), we get $n \simeq 4.2\times 10^5$ s^{-1}. This constancy in ink flux is also adopted in our simulation. In simulation, various deposition rates relative to the diffusion time scale, $n^* = n\Delta t$, are studied (n^* is the number of molecules deposited per time step). For a slowly depositing tip, $n^* < 1$, one ink molecule is deposited for every $1/n^*$ time step (n^* is chosen to give an integer value for $1/n^*$). For a fast deposition case, $n^* > 1$, for every time step n^* molecules are deposited. To do so, for a given lattice position of the tip, $n^* - 1$ nearest neighbor sites of the position are selected. Then n^* ink molecules are given their initial positions at the tip position and its $n^* - 1$ nearest neighbor positions. If the initial lattice position of an ink molecule deposited is unoccupied by other molecules, it is trapped. Otherwise, the molecule is made to execute walking until it is finally trapped by a site previously unoccupied.

III. A CONTINUUM THEORY FOR THE GROWTH OF CIRCLES

For a tip fixed in position, the ink diffusion is isotropic, giving (filled) circles on the surface. Assuming cylindrical symmetry of diffusion and treating the position of ink molecule as continuous variable, we can derive a simple analytic theory for the radial growth of circles. Suppose at time t, the number density at distance r from the tip is given by $P(r,t)$, where $\int 2\pi r P(r,t)dr$ is the total number of molecules deposited until time t. As mentioned in the Introduction, our picture of ink diffusion is that molecules cannot move on the bare surface but can diffuse through the region already covered by other molecules. How the periphery of a circle with radius $R(t)$ varies in time has been known as a moving boundary problem.[11]

Specifically, for a given periphery, $R(t)$, we solve the diffusion equation for the number density within ($r<R$) and outside ($r>R$) the periphery with different diffusion constants D (finite) and $D'(\to 0)$, respectively. At the periphery, $r=R$, the number density is taken to be the monolayer density ρ, and the density flux must be continuous,

$$P(R,t) = P'(R,t) = \rho,$$
$$D\frac{\partial P}{\partial r} = D'\frac{\partial P'}{\partial r}, \tag{3.1}$$

where $P(r,t)$ and $P'(r,t)$ are the densities within and outside the periphery, respectively.

This kind of boundary growth has been solved for various geometries of boundary including spheres,[14,15] cylinders,[15] ellipsoids.[16–19] The derivation of the solution for our particular problem closely follows Carslaw and Jaeger,[12] but is presented here for completeness. $P(r,t)$ and $P'(r,t)$ (Ref. 12) both are given by the exponential integral functions $Ei(-r^2/4Dt)$ and $Ei(-r^2/4D't)$, respectively.[20] In order for the first boundary condition in Eq. (3.1) to be met for all t, $R(t)$ must take the form

$$R(t)^2 = \lambda^2 4Dt. \tag{3.2}$$

Assuming a source depositing n ink molecules per unit time, we impose a constant flux, n, at the origin,

$$-2\pi r D\frac{\partial P}{\partial r}\bigg|_{r\to 0} = n. \tag{3.3}$$

Then the number densities inside and outside the boundary are given by

$$P(r,t) = \rho - \frac{n}{4\pi D}[Ei(-r^2/4Dt) - Ei(-\lambda^2)], \tag{3.4}$$

and

$$P'(r,t) = \frac{\rho}{Ei(-\lambda^2 D/D')}Ei(-r^2/4D't). \tag{3.5}$$

Due to the continuity of the flux at R, Eq. (3.1), λ^2 should satisfy

$$-\frac{n}{4\pi}e^{-\lambda^2} = D'\rho\frac{e^{-\lambda^2 D/D'}}{Ei(-\lambda^2 D/D')}. \tag{3.6}$$

Finally taking the limit $D' \to 0$ and using the asymptotic expansion of $Ei(-x)$ for large x, $Ei(-x) \simeq -e^{-x}/x$, the above equation simplifies to

$$e^{-\lambda^2} = \frac{4D}{(n/\pi\rho)}\lambda^2. \tag{3.7}$$

Equations (3.2), (3.4), and (3.7) form the central results of the continuum theory.

The solution for $R(t)^2$, Eq. (3.2), together with Eq. (3.7) clearly shows how the circle growth is related to the deposition rate, n, and the diffusion constant, D. Note, in Eq. (3.7), $4D$ is the time growth rate of distance squared due to simple (without trapping) diffusion and $n/\pi\rho$ is the growth rate due to deposition when the diffusion takes place instantaneously (diffusion constant infinity). λ^2 is determined by relative magnitude of those two rates. Two limiting cases of the radial growth can be considered. To do so, we first take the logarithm of Eq. (3.7),

$$-\lambda^2 - \ln\lambda^2 = \ln\left[\frac{4D}{(n/\pi\rho)}\right]. \tag{3.8}$$

In the slow deposition limit ($n/\pi\rho \ll 4D$), λ^2 gets very small so that λ^2 in Eq. (3.8) can be neglected to give

$$R(t)^2 = \frac{n}{\pi\rho}t. \tag{3.9}$$

Then the radial growth is solely determined by the deposition rate. On the other hand, in the fast deposition limit ($n/\pi\rho \gg 4D$), λ^2 gets large and now $\ln\lambda^2$ in Eq. (3.8) becomes negligible compared to λ^2, leading to

$$R(t)^2 = 4Dt\ln[(n/\pi\rho)/4D]. \tag{3.10}$$

IV. RESULTS

A. Properties of circles

Our analysis starts with patterns generated by a tip fixed in position on the lattice (simulating DPN result shown in the inset of Fig. 2). Figure 3 shows eight snapshots of circles for slow, $\ln n^* = -2$ (top), and fast, $\ln n^* = 2$ (bottom), deposition cases. To produce the figure, the total time taken for all the molecules to be trapped by lattice sites has been divided into eight equally spaced time intervals. Then in the ascending order of their trapping times, the site positions at which molecules are trapped are drawn as circles, filled circles, squares, filled squares, diamonds, filled diamonds, triangles, and filled triangles. The circle growth is largely isotropic, but, due to the diffusional nature of self-assembly, the periphery is rather noisy. For slow deposition (top), the periphery propagates step by step in time. In contrast, the periphery growth for fast deposition (bottom) is confined to one fourth of the total time, giving a negligible growth at later times.

Let us now focus on the dynamic behavior of the average radius of circle, R. In Fig. 4 is shown the growth of the radius squared, $R(t)^2$, of the periphery from deposition of 2500 ink molecules with various deposition rates ($\ln n^* = -3, -2, -1, 0, 1, 2, 3$). The growth gets faster with increasing deposition rate. Two distinct phases of the growth can be recognized: a linear growth of $R(t)^2$ while the tip is in contact with the surface, and thereafter a much slower increase in the radius that eventually stops when all the molecules are adsorbed. Regardless of the deposition rate, the final radius converges to the same value at long times. For slow deposition cases (top), R^2 deviates from the linear increase in time only at the end of the whole process. In contrast, the deviation for the fast deposition (bottom) starts relatively earlier in time. We also checked the increase in the circle size after the tip is removed. From the radius at the end of tip contact and the final radius of circle, we calculated the area increase of circle after the contact. As expected, the increase is negligible for slow deposition, but for fast deposition the increase is significant (77% increase in area for $\ln n^* = 3$).

Our simulation shows that the circle size, R^2, grows linearly in time during the deposition period. This is exactly what is predicted by the continuum theory developed in Sec. III. For a quantitative comparison, $R(t)^2$ from the simulation is fitted to a linear function of t using chi-square-fitting.[13] In the top of Fig. 5, the radial growth rate, $R(t)^2/4Dt$, from simulation is compared with that of the analytic theory, Eq. (3.2), for various deposition rates, $\ln n^*$. The analytic theory agrees very well with simulation regardless of deposition rates. Note also that the simulation without the excluded volume effect closely matches the full simulation and the analytic theory. Thus the excluded volume effect is hardly observable in our simulation, and the sophisticated procedure to account for such effect seems unnecessary. In the bottom of Fig. 5, the full analytic theory is compared with its slow and fast deposition limit expressions, Eqs. (3.9) and (3.10). The slow deposition limit is quantitative for $\ln n^* = -5, -4, -3, -2, -1$, but the fast deposition limit is not realized for the deposition rates considered [for the fast deposition limit to be valid, $\ln(R^2/4Dt)$ should be negligible compared to $R^2/4Dt$, see Sec. III].

Our random walk results, like the DPN experimental results (Fig. 2), do not have the perfect cylindrical symmetry assumed in the analytic theory. Therefore, as we have already seen in Fig. 3, the periphery of the circle fluctuates from a perfect circle. This fuzziness of the circle boundary pertains to the quality of circles generated by DPN, and thus is of practical importance. The first step in quantifying the noncircular property is calculating the average, μ_R, and standard deviation, σ_R, of the distances of the peripheral points (defined as points with less than four nearest neighbors). The next, not so obvious, step is to note that μ_R/σ_R is a good measure of circularity. This size-independent measure grows as a digital object gets more circular (infinity for a circle).[21] Moreover, for an N-side polygon whose peripheral points are uniformly distributed, it has been found that[21]

$$N \simeq 1.3869(\mu_R/\sigma_R)^{0.4721}. \tag{4.1}$$

We adopt N defined by Eq. (4.1) as a measure of circularity. Varying the number of ink molecules deposited and the deposition rates, we first calculated μ_R and σ_R and averaged them over 30 independent runs to get their average values. The average standard deviation was found to be independent of the deposition rate, and its magnitude never exceeded one lattice spacing (ranging from 0.76 to 0.92 lattice spacings).

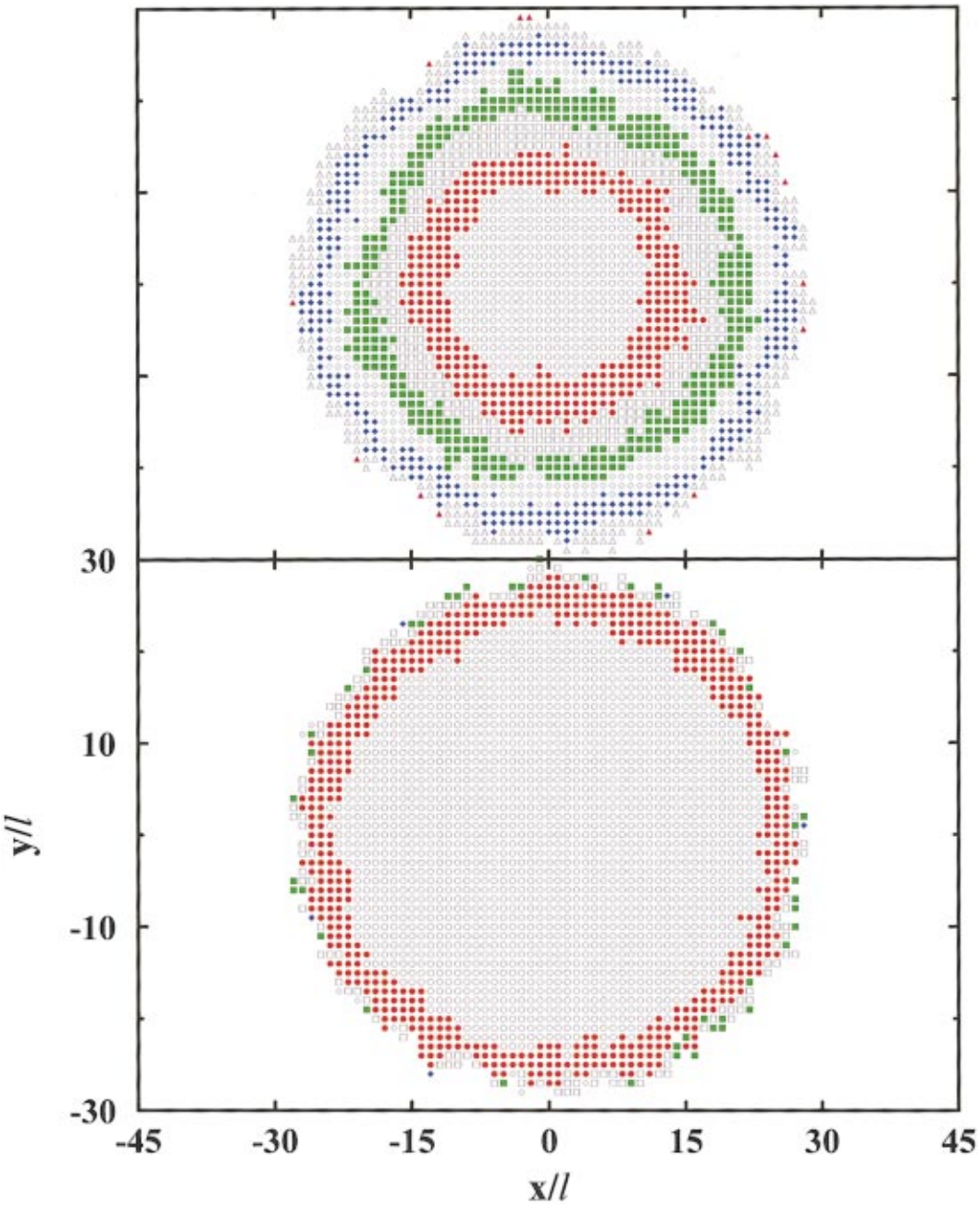

FIG. 3. (Color) Snapshots of circles generated by a tip fixed in position (at $x=0,y=0$ in the figure). We divided the time taken for all the molecules to be trapped into eight equal intervals. In the ascending order of their trapping times, molecules are drawn as circles, filled circles, squares, filled squares, diamonds, filled diamonds, triangles, and filled triangles. Slow, $\ln n^*=-2$ (top), and a fast, $\ln n^*=2$ (bottom), deposition cases are plotted for deposition of 2500 ink molecules.

This small deviation in radius regardless of the deposition rates results from the trapping property of our lattice sites, and contrasts with that of a normal, fluidlike diffusion where molecules can travel everywhere without being trapped. We plot in Fig. 6 the average of circularity (from 30 runs), Eq. (4.1), as a function of number of molecules deposited and deposition rate, $\ln n^*$. Peripheries get more circular with increasing the number of molecules (thus increasing the size of circle). For a given number of molecules deposited, the circularity is fairly constant regardless of deposition rate.

B. Patterns generated by a moving tip

For a tip fixed in space, the results in Sec. IV A show that, by and large, the final structure (characterized by circularity) of the circle generated by DPN seems to be insensitive to whether the ink is deposited fast or slow relative to diffusion time scale of molecules. To generate lines or various structures other than circles in DPN however, the tip has to move across the surface. In this section, we study the effects of the speed of the moving tip and deposition rate on various patterns.

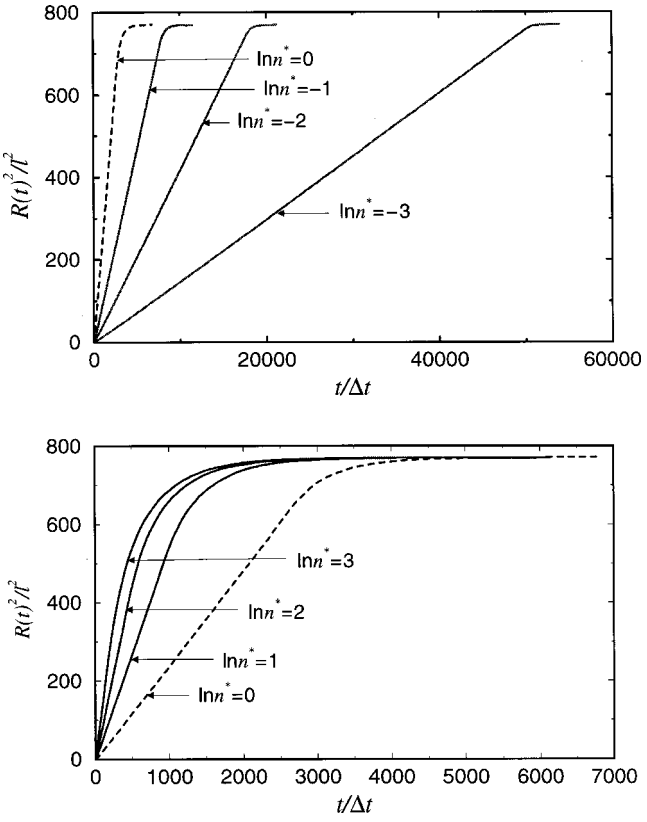

FIG. 4. Radial growth of peripheral points of circles. The radius squared of the periphery, $R(t)^2$, is plotted as a function of time t relative to diffusion time scale, Δt. Slow, $\ln n^*=-3,-2,-1$ (top), and fast, $\ln n^*=3,2,1$ (bottom), deposition cases are plotted separately. The dashed lines drawn in both figures are for $n^*=1$. The radius grows faster with increasing the deposition rate. Total of 2500 ink molecules are deposited, and 10 independent simulations are run to get the average of $R(t)^2$.

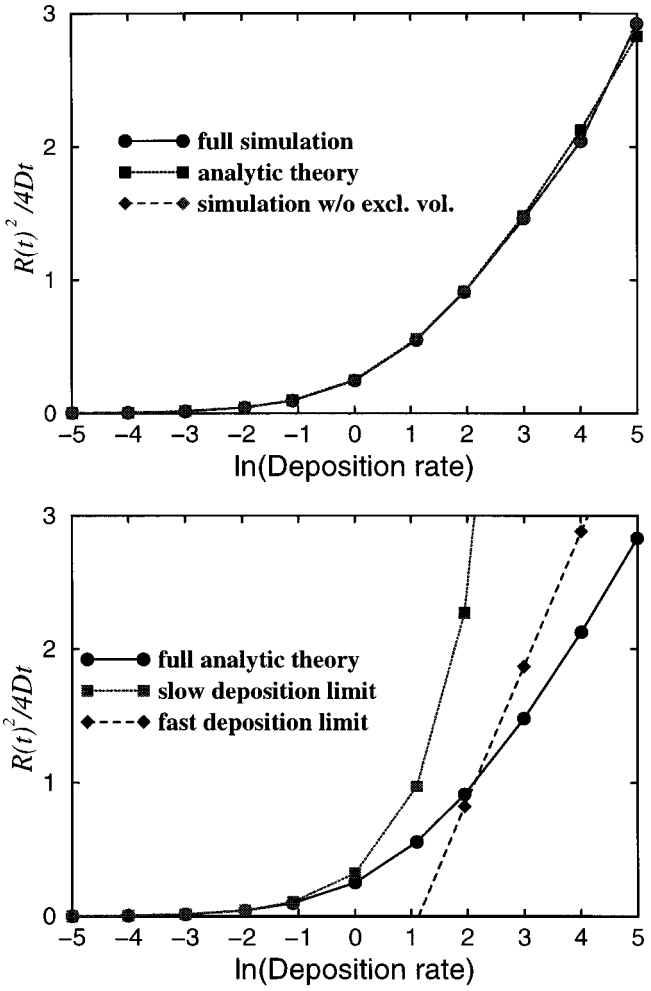

FIG. 5. Radius growth rate in time for various deposition rates, $\ln n^*$. In the top, numerical simulation with or without excluded volume effect is compared to the analytic theory. Drawn in the bottom are the full analytic theory and its limiting expressions in the slow and fast deposition limits. Simulation results are obtained as follows: We first calculated the distances of peripheral points for each time step t_i for deposition of 7000 molecules, and made 20 independent runs to get the average circle radius for each time step, $R(t_i)$. Then the average radius is fitted as $R(t_i)^2=a+bt_i$ (see Ref. 13) and the radial growth rate in the figure is obtained as $b/4D$. The average deviation of the fit, defined as $(1/M)\Sigma_{i=1}^{M}|(R(t_i)^2-a-bt_i)/R(t_i)^2|$ (M=number of data points), was less than 0.044 for all the deposition rates considered.

As a starting point, we checked line segments generated by various tip speeds for a given deposition rate, $n^*=1$. For this deposition rate, we could draw a perfect line by depositing one molecule at each lattice site ($v^*=1$). As we move the tip slower, $\ln v^*=-2$ and -1, we observed broader and fuzzy lines. On the other hand, increasing the tip scan rate, $\ln v^*=2$ and 1, yielded lines which are no longer continuous and look like separated dots aligned straight. A similar trend can be found for more sophisticated patterns such as letters. In Fig. 7(A), for a fixed deposition rate, $\ln n^*=1$, letters N, U, and + are drawn by varying the tip speed as $\ln v^*=-2$ (top), 0 (middle), 2 (bottom). The N and U are drawn by moving the tip without detaching the tip from the lattice until the tip reaches the final lattice points of the letters, but the + is written by first drawing the horizontal line, then detaching the tip and finally drawing the vertical line. Increasing the tip scan rate from $\ln v^*=-2$ to 0 makes the line widths of letters narrower, but further increasing the tip speed makes the points in the letters isolated. Note also that, for the slow tip (top), blurring of the letter + is more prominent at the crossing point of the vertical and horizontal lines. At the crossing, molecules have to be deposited on top of the molecules previously deposited. Thus, molecules dropped later must diffuse over the layer of molecules previously deposited, resulting in the extra blurring seen in the figure. For a qualitative comparison, we show in Fig. 7(B) the lateral force microscope image of 16-mercaptohexadecanoic acid (MHA) monolayer generated by DPN on Au(111) surface. What happens if we fix the tip scan rate and vary the deposition rate? By fixing the tip scan speed to $\ln v^*=-1$, we checked how the letters in Fig. 7(A) change for various deposition rates, $\ln n^*=2$, 0, -2. A slower deposition yielded a narrower linewidth in letters, and we observed patterns nearly identical to those in Fig. 7(A).

Consider a tip scanning a line of certain length as many times as needed to deposit a given amount of molecules. One can then imagine slowly scanning the line once or fast scanning the line over and over again. We here study the effects of tip scan speed and deposition rate on the linewidth; a tip is made to scan a straight line with a length of 31 lattice points until it drops a total of 12 400 ink molecules. The number of

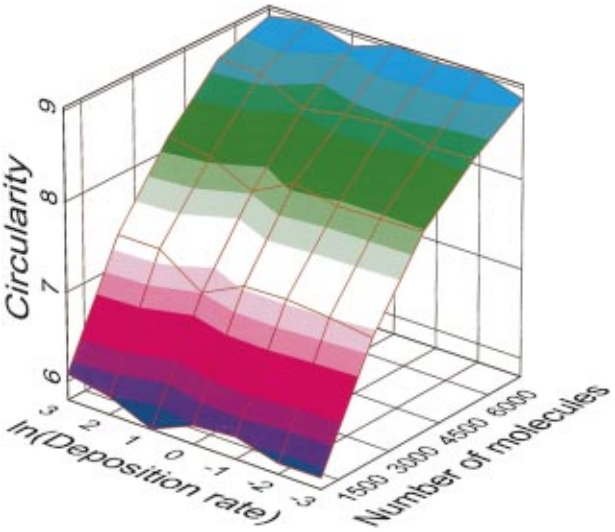

FIG. 6. (Color) The circularity as a function of deposition rate, $\ln n^*$, and the number of molecules deposited. The circularity, defined in Eq. (4.1), is the effective number of sides of a polygon resembling the periphery of circle. For a perfect circle, the circularity is infinity. 30 independent runs were used for calculating each circularity.

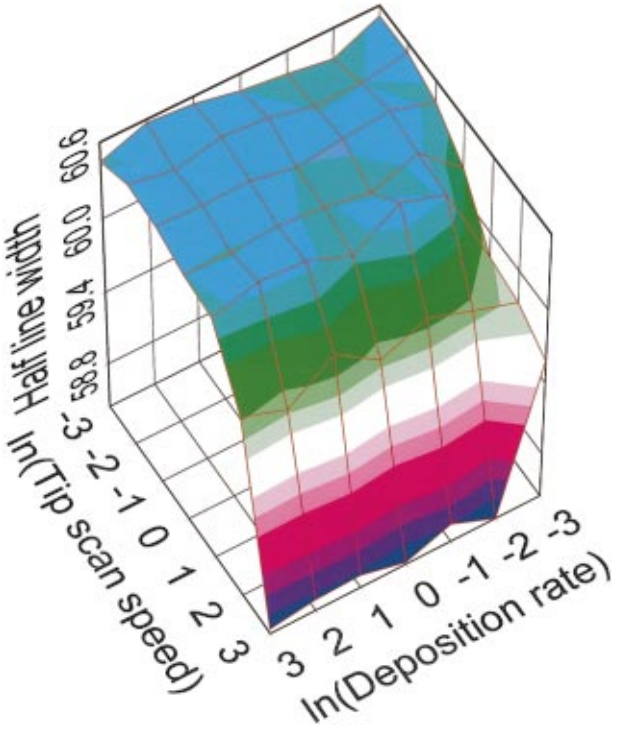

FIG. 8. (Color) Average half linewidth for lines generated by tips with various deposition rates, $\ln n^*$, and tip scan speeds, $\ln v^*$. The linewidth in the figure is given in terms of number of lattice spacings. The tip scanned a straight line with a length of 31 lattice points, and 12 400 ink molecules are deposited. The average was taken over 30 independent runs for each n^* and v^*.

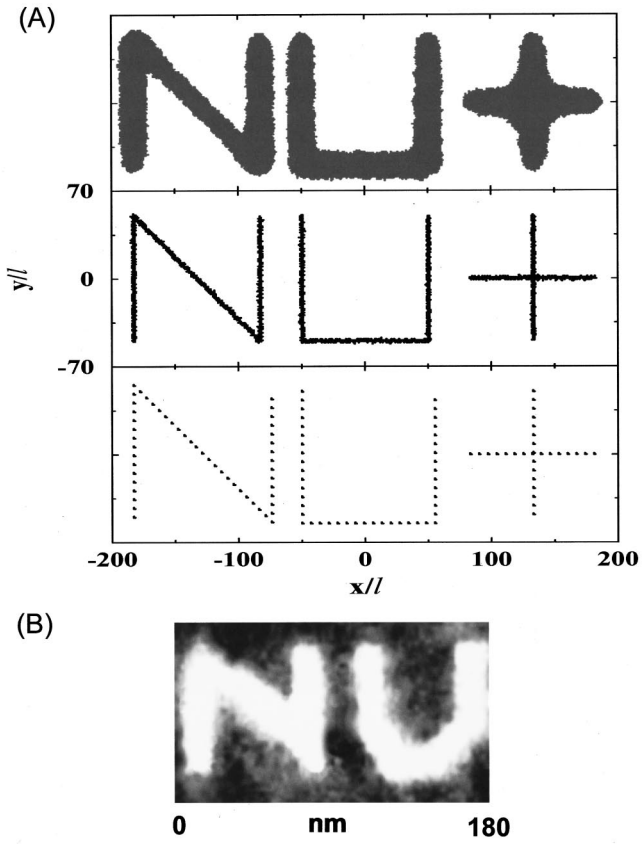

FIG. 7. (A) Letters generated by using various tip scan rates for a fixed deposition rate. For a deposition rate, $\ln n^*=1$, letters are drawn by using different tip scan rates, $\ln v^*=-2$ (top), 0 (middle), 2 (bottom). (B) An AFM image of letters prepared by DPN experiment on Au(111) surface. The letters are made of monolayer thick 16-mercaptohexadecanoic acid (MHA) deposited by using tip scan speed 2 nm/s at relative humidity 23% (at room temperature and under atmospheric condition). The lines in the image are about 15 nm wide. See Ref. 2 for more details.

molecules is chosen so that the slowest tip ($\ln v^*=-3$) with the highest deposition rate ($\ln n^*=3$) considered scans the line just once. The tips with other n^* and v^* then scan the line repeatedly until they use up the same number of ink molecules. The half linewidth is defined as the average distance of peripheral points (again defined as points with less than four nearest neighbors) perpendicular to the scanning line. In Fig. 8, the widths of lines averaged over 30 independent runs are plotted for varying deposition rate and tip scan speed. Increasing the tip scan rate yields a reduced line width, but the actual variation is very small. To see how fuzzy the periphery of the line is, we examined the standard deviation of the distances of peripheral points (perpendicular to the line of scan) from the average half linewidth. We found that the average deviation is about one lattice spacing, and independent of v^* and n^*.

Ink molecules in our model are irreversibly trapped by lattice sites and thus cannot diffuse on the bare surface. This view stresses the strong chemical bond formed between molecules and the surface. In real experiments however, a small but finite mobility of molecules on the bare surface is expected due to the finite strength of chemical bonding. We here examine how the patterns change as we allow for diffusion on the bare surface. In Fig. 9, we plot the circles generated when molecules diffuse on the bare surface with various diffusivities. We have considered the cases where the bare surface diffusion is 10 to 1000 times slower than that on the monolayer of ink molecules. An immediate consequence of the bare surface diffusion is that any pattern deposited will

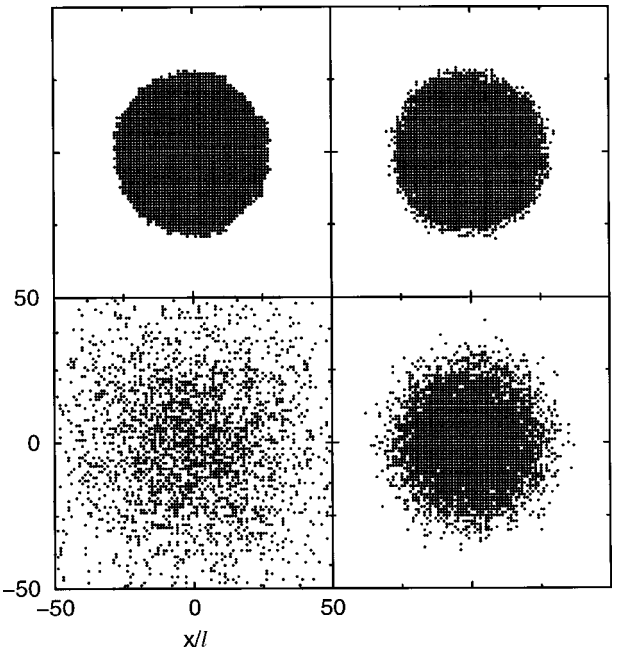

FIG. 9. Circles generated by using various diffusivities on the bare surface. Clockwise starting from the top left, we plot circles generated for bare surface diffusions which are infinitely (no diffusion), 1000, 100, and 10 times slower than the diffusion on the monolayer of molecules. Total of 2500 molecules are deposited, and shown in the figure are snapshots of circles taken at the time when all the molecules are trapped for the case where no bare surface diffusion is allowed.

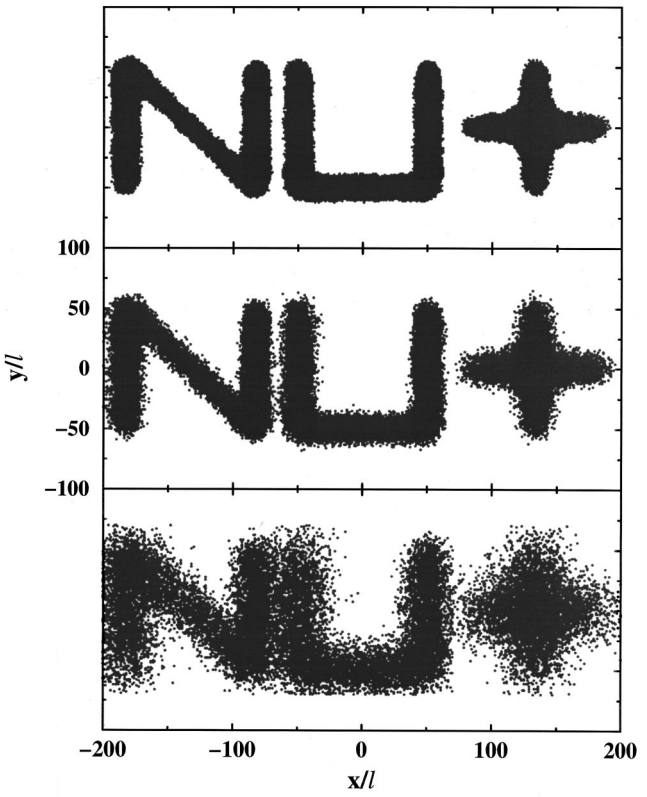

FIG. 10. Letters drawn by allowing the bare surface diffusion. We used the same tip scan speed and deposition rate ($\ln v^*=-2$ and $\ln n^*=1$) as used to generate the top panel of Fig. 7(A). The bare surface diffusivity is varied as 1000 (top), 100 (middle), and 10 (bottom) times smaller than the diffusivity on the monolayer of molecules. For each letter, a snapshot is taken at the time when all the ink molecules deposited are trapped in the case of no bare surface diffusion.

eventually diffuse over the entire surface, yielding no distinct patterns at very long times. Drawn in the figure are snapshots taken at the time when a stable circle forms in the case where no bare surface diffusion is allowed. As we increase the bare surface diffusivity, circles get more and more diffuse in shape. For the bare surface diffusion 10 times slower than that over the monolayer, the circle structure is almost invisible. A similar trend can be found for letters drawn in Fig. 10. Using the same tip speed and deposition rate as used to draw the top panel of Fig. 7(A), the bare surface diffusivity relative to the diffusivity over monolayer is varied as 1/1000 (top), 1/100 (middle), and 1/10 (bottom). Letters get more ill-defined as the bare surface diffusivity is enhanced.

C. Connection to experiments

We have studied patterns formed in DPN under a variety of conditions specified by the tip speed and deposition rate. Every quantity calculated in the simulation is given in terms of the diffusion time scale, Δt, given by Eq. (2.1) and the grid length of the square lattice, l. For the purpose of extracting the qualitative behavior of DPN, our previous analysis is enough. A question that arises is which regime in our simulation corresponds to a real DPN experiment using a specific ink molecule and substrate surface? To make this connection with experiment, we need to identify the basic quantities in our simulation, Δt and l. The grid length, l, in our simulation is taken to be the distance between adsorbed ink molecules, and can be easily identified once the self-assembled monolayer structure is known. With a known grid length, the diffusion time scale can be drawn from the diffusion constant, D, which is related to Δt by Eq. (2.1). So far, DPN experiments have not measured the diffusion constant, and it is not so clear how to measure it (remember the diffusion constant needed is not for diffusion over a bare surface but rather for diffusion over a monolayer of ink molecules).

We here take a specific example, ODT on Au(111), to present our scheme, but the procedure described is generally applicable. Since ODT forms a hexagonal monolayer with a spacing 5 Å on the Au(111) surface,[4,22] we take our grid length as $l=5$ Å. With this grid length, the upper limit of the diffusion constant can be estimated; for our diffusion picture to make sense at all, the diffusion time step must be much larger than the velocity relaxation time. Assuming thermal equilibrium in the velocity distribution, we get[23]

$$\Delta t \gg mD/k_BT, \tag{4.2}$$

where m, T, and k_B are the mass of ODT molecule ($=4.76\times10^{-25}$ kg), temperature, and Boltzmann's constant, respectively. At room temperature $T=298$ K (which is a normal condition for DPN), Eqs. (2.1) and (4.2) give us

$$D \ll 2.32\times10^{-4}\ \text{cm}^2\,\text{s}^{-1}, \quad \Delta t \gg 2.7\ \text{ps}. \tag{4.3}$$

Another estimate of D can be extracted from the diffusivity of eicosanethiol obtained from fitting patterns in microcontact printing. The reported diffusivity[7] is that of the thiol diffusing on a stamp, polydimethylsiloxane (PDMS),

which is taken to be identical to that of eicosanethiol diffusing over a monolayer of the thiol. Using the diffusivity, $D = 7 \times 10^{-8}$ $\mathrm{cm}^2\,\mathrm{s}^{-1}$, along with the deposition rate, n, and the lattice spacing l already calculated for ODT on Au (111), we get the diffusion time scale of $\Delta t = 8.9$ ns. Assuming a typical tip scan speed, $v = 1$ μm/s, we get $\ln n^* = -5.6$ and $\ln v^* = -10.9$, which corresponds to a slow deposition and tip scan relative to the diffusion time scale.

V. SUMMARY AND CONCLUSION

In this paper, we have presented the first theoretical study on the self-assembly of ink molecules in DPN. The dynamics of the self-assembly has been modeled as a two dimensional random walk on a square lattice. The flow of ink from the tip is approximated as a constant flux of molecules. To mimic the chemisorption of ink molecules to the substrate, it is assumed that every site on the lattice traps a molecule, and molecules diffuse only over the region previously covered by other molecules. It is shown that the growth of patterns can be viewed as a phase growth with a source, and the circle growth in DPN reduces to a well-known problem in theories of diffusional phase growth. An analytic solution for the circle growth has been presented and shown to agree well with simulation.

Varying the magnitudes of deposition rate and tip scan speed relative to the diffusion time scale of ink molecules, we have studied the patterns generated by DPN. The peripheries of circles and lines have been characterized by circularity and linewidth, respectively. For a fixed tip, the resulting circles are insensitive to the deposition rate as long as the same number of molecules are deposited, but increasing the total number of molecules yielded more circular patterns. Patterns created by a moving tip significantly depended on the tip speed and deposition rate. Although fast scan or slow deposition generally enhances the resolution of patterns, further increasing scan rate (or decreasing deposition rate) could result in disconnected patterns. It is actually difficult to analyze more complex patterns such as blurred crossing points or rounded corners of letters just in terms of linewidth or circularity. Then it would be necessary to look at another aspect of the patterns such as connectivity and convexity.[24] To apply our results to a specific experiment, knowledge of the diffusion constant is crucial. We have considered possible values which D may have. These indicate that deposition and scanning are slow compared to diffusion, but this estimate is very uncertain. Fortunately, many of the results are relatively insensitive to the deposition rate or scan rate, so this uncertainty is not crucial to the conclusions of this work.

Even for the perfect crystalline surface studied here, DPN patterns have a random periphery due to the diffusional nature of self assembly. In addition to this diffusional blurring of patterns, the surface itself might be corrugated, polycrystalline, anisotropic and have defects in binding sites due to contamination. These extra factors are expected to further deteriorate the quality of DPN results. It would be interesting to study exactly how the quality of substrate plays a role in the resolution of DPN. Lastly, we hope to understand the microscopic details of ink deposition from the tip to the substrate. Is water condensation, if it forms at all, really triggering the ink transport from the tip? What does the water meniscus look like and what controls the narrowness of the ink flow? Will the ink flux be constant in time on a molecular diffusion time scale? These are the questions we hope to answer in the near future.

ACKNOWLEDGMENTS

The authors are grateful to DOD/MURI for support of this work and Chad Mirkin for valuable suggestions. One of the authors (J.J.) thanks Dr. Jaeyoung Sung for helpful discussions.

[1] S. Hong and C. A. Mirkin, Science **288**, 1808 (2000).
[2] S. Hong, J. Zhu, and C. A. Mirkin, Science **286**, 523 (1999).
[3] S. Hong, J. Zhu, and C. A. Mirkin, Langmuir **15**, 7897 (1999).
[4] R. D. Piner, J. Zhu, F. Xu, S. Hong, and C. A. Mirkin, Science **283**, 661 (1999).
[5] R. D. Piner and C. A. Mirkin, Langmuir **13**, 6864 (1997).
[6] D. A. Weinberger, S. Hong, C. A. Mirkin, B. W. Wessels, and T. B. Higgins, Adv. Mater. **12**, 1600 (2000).
[7] E. Delamarche, H. Schmid, A. Bietsch, N. B. Larsen, H. Rothuzien, B. Michel, and H. Biebuyck, J. Phys. Chem. B **102**, 3324 (1998).
[8] A. Bernard, J. P. Renault, B. Michel, H. R. Bosshard, and E. Delamarche, Adv. Mater. **12**, 1067 (2000); H. Kind, M. Geissler, H. Schmid, B. Michel, K. Kern, and E. Delamarche, Langmuir **16**, 6367 (2000).
[9] J. L. Wilbur, A. Kumar, E. Kim, and G. M. Whitesides, Adv. Mater. **6**, 600 (1994); Y. Xia and G. M. Whitesides, J. Am. Chem. Soc. **117**, 3274 (1995).
[10] R. Mahaffy, R. Bhatia, and B. J. Garrison, J. Phys. Chem. B **101**, 771 (1997).
[11] J. Crank, *The Mathematics of Diffusion*, 2nd ed. (Oxford University Press, London, 1975).
[12] H. S. Carslaw and J. C. Jaeger, *Conduction of Heat in Solids* (Oxford University Press, London, 1959).
[13] W. H. Press, S. A. Teukolsky, W. T. Vetterling, and B. P. Flannery, *Numerical Recipes in Fortran 90* (Cambridge University Press, Cambridge, 1996). We used the numerical routine **fit**.
[14] C. Zerner, J. Appl. Phys. **20**, 950 (1949).
[15] F. C. Frank, Proc. R. Soc. London, Ser. A **201**, 586 (1950).
[16] G. P. Ivantsov, Dokl. Akad. Nauk SSSR **58**, 567 (1947).
[17] F. S. Ham, J. Phys. Chem. Solids **6**, 335 (1958).
[18] F. S. Ham, Q. Appl. Math. **17**, 137 (1959).
[19] G. Horvay and J. W. Cahn, Acta Metall. **9**, 695 (1961).
[20] M. Abramowitz and I. A. Stegun, *Handbook of Mathematical Functions* (Dover, New York, 1970).
[21] R. M. Haralick, IEEE Trans. Syst. Man Cybern. **SMC-4**, 394 (1974).
[22] C. A. Alves, E. L. Smith, and M. D. Porter, J. Am. Chem. Soc. **114**, 1222 (1992).
[23] S. Chandrasekhar, in *Selected Papers on Noise and Stochastic Processes* (Dover, New York, 1954).
[24] A. Rosenfield and A. C. Kak, *Digital Picture Processing* (Academic, New York, 1976).